Franck–Condon profiles in photodetachment-photoelectron spectra of HS_2^- and DS_2^- based on vibrational configuration interaction wavefunctions

Joonsuk Huh, Michael Neff, Guntram Rauhut, Robert Berger

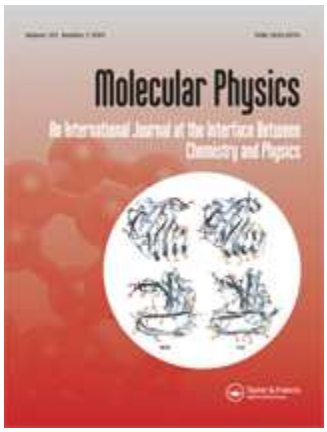

Franck--Condon profiles in photodetachment-photoelectron spectra of HS$_2^-$ and DS$_2^-$ based on vibrational configuration interaction wavefunctions

Journal:	*Molecular Physics*
Manuscript ID:	TMPH-2009-0292.R1
Manuscript Type:	Special Issue Paper - In honour of Prof Werner 60th birthday
Date Submitted by the Author:	25-Nov-2009
Complete List of Authors:	Huh, Joonsuk; Johann Wolfgang Goethe University, Frankfurt Institute for Advanced Studies Neff, Michael; University of Stuttgart, Institute of Theoretical Chemistry Rauhut, Guntram; Universitity of Stuttgart, Institute of Theoretical Chemistry Berger, Robert; Johann Wolfgang Goethe-University, Frankfurt Institute for Advanced Studies (FIAS)
Keywords:	Franck-Condon, VSCF/VCI, photodetachment-photoelectron spectra, CCSD(T)-F12, HS$_2$
Note: The following files were submitted by the author for peer review, but cannot be converted to PDF. You must view these files (e.g. movies) online.	
New WinZip File.zip	

Franck–Condon profiles in photodetachment-photoelectron spectra of HS_2^- and DS_2^- based on vibrational configuration interaction wavefunctions

Joonsuk Huh,[1] Michael Neff,[2] Guntram Rauhut,[2,*] and Robert Berger[1,†]

[1]*Frankfurt Institute for Advanced Studies, Johann Wolfgang Goethe-University, Ruth-Moufang-Str. 1, 60438 Frankfurt, Germany*

[2]*Institut für Theoretische Chemie, Universität Stuttgart, Pfaffenwaldring 55, 70569 Stuttgart, Germany*

Abstract

Explicitly electron correlating coupled cluster calculations, CCSD(T)-F12a, were performed to determine three-dimensional potential energy hypersurfaces of disulfanide and disulfanyl in an automated approach. Surfaces for different electronic states were used in a Watson rovibrational Hamiltonian ansatz to obtain the correlated anharmonic vibrational wavefunctions. Subsequently the anharmonic Franck–Condon overlap integrals were evaluated. The computed Franck–Condon profiles were compared to experimental photodetachment-photoelectron spectra and confirm essentially the assignments made previously. The profiles indicate, however, additional weaker, and as of yet unresolved, additional features.

Dedicated to Prof. H.-J. Werner on the occasion of his 60th birthday.

I. INTRODUCTION

Quite recently, Entfellner and Boesl[1] have reported an experimental photodetachment-photoelectron study of the HS_2^- and DS_2^- isotopomers of disulfanide in which the disulfanyl isotopomers HS_2 and DS_2 were obtained in different electronic states. A resolution of $\approx$ 160 cm^{-1} was achieved in this study. The interpretation and assignment of the spectra was supported by an earlier photoelectron spectroscopic investigation by Moran and Ellison.[2] In addition, the work presented there was also guided by previous theoretical studies of Peterson *et al.*[3] who computed many vibrational transitions for HS_2 and DS_2 at the highest computational levels but did not consider the corresponding anions. The intensity profile of the photodetachment-photoelectron spectra, however, was only indirectly exploited in the analysis of Entfellner and Boesl, but not directly compared to an accurate calculation of the vibronic spectral shape for the photodetachment process.

Calculations of (harmonic and anharmonic) vibronic transition profiles in polyatomic molecules, in particular within the Franck–Condon (FC) approximation, have a long history (see *e.g.* Refs. 4–8 and literatur cited in Ref. 9). In the past decade, one of the areas of activity was to incorporate efficiently the Duschinsky mode mixing effects[10] in the computation of harmonic spectral profiles of large molecular systems (see e.g. Refs. 9,11 and literature cited therein). Another was the inclusion of anharmonicities in FC profile calculations of small (triatomic) up to medium sized (9-atomic) systems (see e.g. Refs. 12–17 and literature cited therein). Initially the use of specifically tailored vibrational coordinates and corresponding one particle basis functions, that try to minimize the couplings in the potential energy terms, was widespread due to limited computational resources. Nowadays, there appears to be a trend towards brute-force application of general sets of coordinates that often involve normal coordinates in terms of Cartesian displacements, at least when relatively rigid molecules are considered[18–21]. This facilitates the more or less automated calculation of anharmonic vibronic spectra by combining electronic and vibronic structure codes, however typically at the price of higher computational cost.

For instance Mok *et al.*[12] used individual (Duschinsky rotated) harmonic oscillator basis functions for each electronic state and expanded the anharmonic wavefunction of each state in this basis. Due to the Duschinsky effect, the basis functions of two electronic states are, in general, non-orthogonal and this necessitates the explicit calculation of the corresponding

overlap integrals. The authors employed the Watson rovibrational Hamiltonian in their calculations, which have, up to now, primarily been performed for various non-linear triatomic molecules.

Bowman *et al.*[14] used vibrational self-consistent field (VSCF) and vibrational configuration interaction (VCI) methods together with the Watson Hamiltonian to compute FC factors (FCFs). They employed, however, one set of primitive harmonic oscillator basis functions for both states, which renders the computation of their corresponding overlap integrals trivial but typically requires much longer VCI expansions to describe accurately the intensity profile near the origin of the vibronic band (0'-0 transition region).

Luis *et al.*[13,22] used either vibrational perturbation theory or VSCF/VCI functions, apparently only for the final electronic state, and determined the Franck–Condon factors by solving subsequently a homogeneous linear system of equations. They employed, however, only a simple diagonal kinetic energy operator without vibrational angular momentum terms and without the Watson correction term. These authors have reported applications even to systems with nine atoms, although with a significantly reduced set of mode-mode couplings.

Rodriguez-Garcia *et al.*[15] also used this simplified kinetic energy operator and compared two types of approaches, namely (i) the use of harmonic oscillator basis functions adapted to each electronic state involved, which thereby require to compute overlap integrals between distorted, displaced and rotated harmonic oscillators, and (ii) VCI calculations using a common set of basis functions for both electronic states. The vibronic spectra of the systems studied, however, were largely dominated by the 0'-0 transition which thus seems to be a particularly favourable situation for a common basis set.

The photodetachment process of disulfanide can (depending on the final electronic state) be accompanied by a relatively large change in the equilibrium structure due to the shortening of the S-S bond length ($\Delta r_{\mathrm{S-S}} \sim 0.1$ Å), as a relatively long vibrational progression is visible in the corresponding photoelectron spectrum of the anion, thereby posing a problem which appears somewhat better suited for computational methods that employ individual vibrational basis functions for the vibrational motion in the initial and final electronic states.

We thus present herein our integrated vibronic structure approach for the calculation of the FC profile of the photodetachment-photoelectron spectra. This approach, which we will outline in the next section, shares some features of the one by Mok *et al.*[12], in that we are using separate sets of basis functions in the two electronic states and employing the Watson

rovibrational Hamiltonian including the pseudopotential-like Watson correction term and the vibrational angular momentum terms for the solution of the vibrational problem. As in most previous work, all additional angular momentum coupling terms like electron spin-rotational, electron spin-electron orbit and nuclear rotation-electron orbit couplings were dropped. However, these are necessary for high-accuracy benchmark calculations of vibrational wavenumbers, see for example the work of Werner and others on the water cation[23]. We deviate from the ansatz of Mok *et al.* by using a VSCF/VCI ansatz for the description of the numerous vibrational wavefunctions and by employing for each electronic state a separate set of distributed Gaussians as primitive basis functions for the VSCF calculations. The latter functions allow, due to their locality, simple prescreening strategies in the calculation of the FC integrals of n-dimensional anharmonic oscillators to be exploited. Potential energy surfaces are obtained by making use of a fully automated surface construction code[24,25] (see below). For the present application, the potential energy surfaces were computed at the (U)CCSD(T)-F12a/vtz-f12 level.

II. THEORY

As outlined above our approach for obtaining vibrational wavefunctions is based on the Watson Hamiltonian[26] for polyatomic non-linear molecules.

$$\hat{H} = \frac{1}{2}\sum_{\alpha\beta}\hat{\pi}_\alpha\mu_{\alpha\beta}\hat{\pi}_\beta - \frac{1}{8}\sum_{\alpha}\mu_{\alpha\alpha} - \frac{1}{2}\sum_{i}\frac{\partial^2}{\partial q_r^2} + V(q_1,\ldots,q_{3N-6}) \tag{1}$$

Like the potential, the 2nd term, the so-called Watson correction term, is represented in a many-mode expansion and is added as a pseudopotential-like contribution to the potential $V(q_1,\ldots,q_{3N-6})$ expressed in normal coordinates q_i. For details see Ref. 24. We used a distributed Gaussian basis χ_μ

$$\chi_\mu(q) = \sqrt[4]{\frac{2A_\mu}{\pi}}\exp\{-A_\mu(q-q_\mu)^2\} \tag{2}$$

for representing the one-mode wavefunctions $\phi_i(q_i)$ (modals) within the VSCF and VCI approaches. The parameters A_μ were determined as described in the seminal paper of Hamilton and Light[27]. As normal modes are distinguishable, the VSCF many-mode wavefunction Φ can be expressed as a simple Hartree product of the modals, *i.e.*

$$\Phi^{(\mathbf{n})}(\mathbf{q}) = \prod_i \phi_i^{(n_i)}(q_i) \qquad \text{with} \qquad \phi_i^{(n_i)}(q_i) = \sum_\mu C_{\mu i}^{(n_i)}\chi_\mu(q_i) \tag{3}$$

where $\mathbf{n}$ denotes the occupation number vector (ONV) with elements n_i and we assume the expansion coefficients of the modals to be real numbers. The corresponding VCI solution is a simple linear combination of such wavefunctions with different ONVs. Based on a separability approach, the $3N-6$ dimensional eigenvalue problem is reduced to $3N-6$ one-dimensional problems within the VSCF method. Once a polynomial representation of the potential has been chosen, the resulting one-dimensional effective polynomial, $\bar{p}_r^{(i)}$, can be expressed as[28]

$$\bar{p}_r^{(i)} = p_r^{(i)} + \sum_j \sum_s X_{js} \left[p_{rs}^{(ij)} + \sum_k \sum_t X_{kt} \left[\frac{1}{2} p_{rst}^{(ijk)} + \dots \right] \right] \tag{4}$$

where r denotes the order of the polynomial. The effective polynomial exclusively depends on the fitting coefficients p and the one-dimensional potential integrals:

$$Q_{\mu\nu}^r = \langle \chi_\mu | q^r | \chi_\nu \rangle \qquad \text{and} \qquad X_{ir} = \sum_{\mu\nu} C_{\mu i} C_{\nu i} Q_{\mu\nu}^r \tag{5}$$

Note that the integrals $Q_{\mu\nu}^r$ are mode-independent, provided that the same Gaussian basis set is employed for all modes. The VSCF/VCI approach outlined here was successfully used in many applications but usually was limited to the calculation of fundamental modes or low lying overtones and combination bands[29–31].

The basic building block of the vibronic structure calculation with the VSCF and VCI wavefunctions is the overlap integral between rotated, distorted and displaced Gaussian functions. The normal coordinates of the two different electronic states are connected by the Duschinsky relation[10]

$$\mathbf{q}' = \mathbf{S}\mathbf{q} + \mathbf{d} \tag{6}$$

where $\mathbf{S}$ is the Duschinsky rotation matrix and $\mathbf{d}$ is the displacement vector. With the quantities defined by Doktorov *et al.*[32], *i.e.*

$$\mathbf{R} = (\mathbf{I} + \mathbf{J}^{\mathrm{t}}\mathbf{J})^{-1}\mathbf{J}^{\mathrm{t}}, \quad \mathbf{P} = \mathbf{J}(\mathbf{I} + \mathbf{J}^{\mathrm{t}}\mathbf{J})^{-1}\mathbf{J}^{\mathrm{t}}, \quad \mathbf{J} = \mathbf{\Omega}'\mathbf{S}\mathbf{\Omega}^{-1} \quad \text{and} \quad \boldsymbol{\delta} = \mathbf{\Omega}'\mathbf{d} \tag{7}$$

in which $\mathbf{\Omega} = \mathrm{diag}((2A_{\mu 1}), \dots, (2A_{\mu(3N-6)}))^{1/2}$ and $\mathbf{\Omega}' = \mathrm{diag}((2A'_{\mu' 1}), \dots, (2A'_{\mu'(3N-6)}))^{1/2}$, where prime ($'$) is used to specify the parameters belonging to the final electronic state, the multi-dimensional overlap integral (characterised by the vectors $\boldsymbol{\mu}'$ and $\boldsymbol{\mu}$ with elements μ'_i and μ_i, respectively) of the Gaussian basis functions is given as

$$\int \prod_i \chi'_{\mu'_i}(q'_i) \chi_{\mu_i}(q_i) \, \mathrm{d}\mathbf{q} = 2^{(3N-6)/2} \, |\det(\mathbf{R})|^{1/2} \, \exp\left[-\frac{1}{2} \boldsymbol{\delta}^{\mathrm{t}} (\mathbf{I} - \mathbf{P}) \boldsymbol{\delta} \right]. \tag{8}$$

The norm of the overlap integral has a trivial upper bound in the limiting case of identical Gaussian exponent parameters between the initial and final electronic state Gaussian basis set functions and in the absence of Duschinsky rotation, which is

$$\left| \int \prod_i \chi'_{\mu'_i}(q'_i)\chi_{\mu_i}(q_i)\,\mathrm{d}\mathbf{q} \right| \leq \exp\left[-\frac{1}{4}||\boldsymbol{\delta}||^2\right] \tag{9}$$

and only depends on the norm of the delta vector. This simple bound condition is exploited in our overlap integral prescreening and integrals (with norm estimate) below 10^{-8} were ignored.

The VSCF wavefunction overlap integral is expressed in terms of the Gaussian overlap integrals

$$\int \Phi'^{(\mathbf{n}')}(\mathbf{q}')\Phi^{(\mathbf{n})}(\mathbf{q})\,\mathrm{d}\mathbf{q} = \sum_{\boldsymbol{\mu},\boldsymbol{\mu}'} \left(\prod_i C^{(n'_i)}_{\mu'_i} C^{(n_i)}_{\mu_i} \right) \int \left(\prod_i \chi'_{\mu'_i}(q'_i)\chi_{\mu_i}(q_i) \right) \mathrm{d}\mathbf{q}. \tag{10}$$

The VCI wavefunction of the m-th vibrational state is expanded in terms of the VSCF wavefunction with real expansion coefficients $B^{(\vec{n})}_m$

$$\Psi_m(\mathbf{q}) = \sum_{\mathbf{n}} B^{(\mathbf{n})}_m \Phi^{(\mathbf{n})}(\mathbf{q}). \tag{11}$$

With this, the corresponding overlap integrals of the VCI wavefunctions reads as

$$\int \Psi'_{m'}(\mathbf{q}')\Psi_m(\mathbf{q})\,\mathrm{d}\mathbf{q} = \sum_{\mathbf{n},\mathbf{n}'} B'^{(\mathbf{n}')}_{m'} B^{(\mathbf{n})}_m \sum_{\boldsymbol{\mu},\boldsymbol{\mu}'} \left(\prod_i C'^{(n'_i)}_{\mu'_i} C^{(n_i)}_{\mu_i} \right) \int \prod_i \chi'_{\mu'_i}(q'_i)\chi_{\mu_i}(q_i)\,\mathrm{d}\mathbf{q}. \tag{12}$$

In the evaluation of the VCI overlap integral the terms of $B'^{(\mathbf{n}')}_{m'} B^{(\mathbf{n})}_m$ below 10^{-8} were dropped in the summation.

III. COMPUTATIONAL DETAILS

A. Electronic Structure Calculations

Electronic structure calculations were performed at the (U)CCSD(T)-F12a/vtz-f12 level. Explicitly correlated coupled-cluster calculations are much better suited for the generation of accurate potential energy surfaces than conventional (U)CCSD(T) calculations, because less demanding orbital basis sets can be used. This reduces the I/O bottleneck in the corresponding Hartree-Fock calculations, which may be severe once many *ab initio* calculations need to be performed. The RMP2-F12 calculations, which are the first step in

(U)CCSD(T)-F12a calculations, were performed using the MP2-F12/**3**C(FIX) method[33,34]. In this method the numerous two-electron integrals are computed using robust density fitting (DF) approximations[35,36] (DF was not used in the Hartree-Fock and UCCSD(T)-F12 calculations). The aug-cc-pVTZ/MP2FIT basis set of Weigend et al.[37] was used as auxiliary basis. For evaluating the Fock matrix (which is needed in the AO and RI basis sets) the vtz/OPTRI basis sets[38] was employed. The complementary auxiliary basis set (CABS) approach was employed, i.e., the union of the AO and RI basis sets was used to approximate the resolution of the identity. The perturbative CABS singles correction as described in Refs. 39,40 was applied in all F12 calculations. This significantly reduces the Hartree-Fock basis set error. Careful tests showed that the choice of the density fitting basis has only a negligible effect on the vibrational wavenumbers. The choice of the RI basis is more critical; however, we found that employing larger RI basis sets does not reduce the statistical errors. Tight CABS thresholds (10^{-9}) were used in order to minimise the number of functions that are deleted due to near linear dependencies. The number of functions was kept constant for all displacements. This guarantees smooth potential energy surfaces. For an application of explicitly correlated coupled-cluster theory, CCSD(T)-F12, on the calculation of vibrational transitions see Ref. 31.

B. Calculation of Potential Energy Surfaces

Potential energy surfaces were represented by a multi-mode expansion in terms of normal coordinates rather than a Taylor series expansion. These surfaces were generated in a fully automated fashion based on an iterative interpolation algorithm as described in detail elsewhere[24,25]. In a first step all surfaces were represented by 20 grid points in each direction but a subsequent transformation to polynomials up to 8th order was used for the calculation of the fundamental modes[28].

C. VSCF/VCI Calculations

Once the potential had been determined — either in terms of grid points or polynomials — the vibrational self-consistent field approximation was used for calculating the fundamental modes of $HS_2^{0/-}$ and $DS_2^{0/-}$. Each modal was represented by a linear combination of 30

distributed Gaussians. In the VSCF calculations, vibrational angular momentum terms were included perturbatively using the converged VSCF wavefunction and a constant μ-tensor as discussed by Carbonniere and Barone[30,41]. Vibrational correlation effects were included subsequently by vibrational configuration interaction calculations including single, double and triple excitations, leading to a total of 216 VCI states[28]. In the VCI calculations, vibrational angular momentum terms were included variationally.

D. Vibronic Structure Calculations

Franck–Condon factors (FCFs) for the $(\tilde{\mathrm{X}}\ ^1\mathrm{A}')\mathrm{HS}_2^- \rightarrow (\tilde{\mathrm{X}}\ ^2\mathrm{A}'')\mathrm{HS}_2$, $(\tilde{\mathrm{X}}\ ^1\mathrm{A}')\mathrm{HS}_2^- \rightarrow (\tilde{\mathrm{A}}\ ^2\mathrm{A}')\mathrm{HS}_2$, $(\tilde{\mathrm{X}}\ ^1\mathrm{A}')\mathrm{DS}_2^- \rightarrow (\tilde{\mathrm{X}}\ ^2\mathrm{A}'')\mathrm{DS}_2$ and $(\tilde{\mathrm{X}}\ ^1\mathrm{A}')\mathrm{DS}_2^- \rightarrow (\tilde{\mathrm{A}}\ ^2\mathrm{A}')\mathrm{DS}_2$ photodetachment-photoelectron spectra were computed using the VSCF/VCI vibrational wavefunctions obtained as described above and, for comparison, using approximate three-dimensional harmonic oscillator wavefunctions. As these wavefunctions were obtained using normal modes specific for each electronic state, Duschinsky mode mixing effects[10] had to be taken into account. To this end, a development version of the MOLPRO program package[42] used for the electronic and vibrational structure calculations reported herein was interfaced to a development version of the hotFCHT software[9,43,44] which was employed for subsequent vibronic structure studies. VSCF based vibronic spectra reported below were computed by using the modals obtained in a VSCF calculation for the vibrational ground state of each electronic state. Excited vibrational states were approximated within an uncoupled Hartree framework by products involving excited modals obtained in the vibrational ground state SCF procedure and the energies of the various states (including the ground state) were approximated by sums of the corresponding modal energies. None of these vibrational state energies were subsequently corrected perturbatively for angular momentum contributions. Thus, shifts between VSCF and VCI vibronic band positions are due to vibrational correlation effects *and* the vibrational angular momentum terms included in the latter approach but neglected in the former. As the changes in equilibrium structures and normal modes are comparatively large in the $\tilde{\mathrm{X}}\ ^1\mathrm{A}' \rightarrow \tilde{\mathrm{X}}\ ^2\mathrm{A}''$ transitions, the use of specific normal modes appears beneficial as it reduces the length of the VCI expansions (number of VCI basis functions) required to accurately describe the intensity pattern in the 0'-0 transition region. The price to pay is the increased cost in the calculation of individual overlap integrals between basis func-

tions, as the basis functions are non-orthogonal and the corresponding overlap integrals are not separable into simple products of one-dimensional integrals. Prescreening techniques for multidimensional overlap integrals of distributed Gaussians still allow rapid calculation of these integrals such that the reduced expansion lengths may outweight the higher cost. This situation is significantly different from a previous study along similar lines reported by Rodriguez-Garcia *et al.*[15], where the vibronic spectra were largely dominated by the 0'-0 transition band and thus structural changes were also very small. Besides prescreening on the level of multidimensional overlap integrals between Gaussian basis functions (Eq. (10)) and on the level of the VCI expansion coefficients, one can also envisage an additional prescreening stage for the overlap integrals between VSCF wavefunctions (in Eq. (12)) that will also impact on the cross-over point for the common basis set and individual basis set approaches. Low-cost *a priori* estimates of the respective numerical effort would be desirable, but are beyond the scope of the present work.

IV. RESULTS AND DISCUSSION

Bond lengths, harmonic wavenumber and the fundamentals of $HS_2^{0/-}$ and $DS_2^{0/-}$ computed at the VCI level are shown in Tables I and II. With respect to the S-S bond lengths, our UCCSD(T)-F12a/vtz-f12 results deviate slightly from those of Peterson *et al.*[3]. However they do agree nicely with those obtained at the complete basis set limit but without core correlation and and high-order correlation effects, which are not included in our calculations. Except for the H-S-stretching modes our VCI results are in excellent agreement with the computed anharmonic wavenumbers of Peterson *et al.*[3] This holds true in particular for the deuterated species. In general, we consider the results of these authors to be more accurate than our's, because they did not only account for high-order electron correlation effects (in terms of CCSDTQ calculations), but also incorporated core-correlation effects and scalar-relativistic corrections. As our intention is not to reproduce the spectroscopic properties of these molecules most accurately but to study routes for determining the vibrational finestructure of their photodetachment-photoelectron spectra, we did not correct our potential energy surfaces for these effects. However, a comparison of the results of Peterson *et al.* to our's shows that these corrections are usually quite small. In most cases deviations with respect to the experimental values[1] are significantly larger which we attribute to the large

error bar in the experiments. We believe that the accuracy of our calculations is sufficient in order to simulate the vibrational structure of the photodetachment-photoelectron spectra.

The computed Franck–Condon (FC) profiles of the computed ($\tilde{\mathrm{X}}\ ^1\mathrm{A}'$) $\rightarrow$ ($\tilde{\mathrm{X}}\ ^2\mathrm{A}''$) photodetachment-photoelectron of HS_2^- and DS_2^- are displayed in Figs. 1 and 2, respectively. For each of these transitions we show the stick representation for the FC profile (corresponding to the individual FCFs of the various transitions) as well as the FC profile as obtained after convolution with Lorentzian lineshape function with full width at half maximum (FWHM) of 200 cm^{-1}. The full band listing up to 4000 cm^{-1} above the 0'-0 transition wavenumber is reported in the appendix.

For both species the computed main spectral feature of this transition is a pronounced progression 3_0^n in the S-S stretching mode ν_3 that extends (visibly) up to about $n' = 5$. This progression has also been identified by Entfellner *et al.*[1] in the experimental low resolution photodetachment-photoelectron spectrum, with the progression extending as well up to about $n' = 5$. The FCFs of the 3_0^1 and 3_0^2 transition are the largest of the spectrum, with the former being less than 5 % (less than 13%) larger than the latter in HS_2 (in DS_2). The FCFs of the 0_0^0 transition and the 3_0^3 transition are of similar magnitude and both are predicted to be half the size of the 3_0^1 within the VSCF and VCI framework. The harmonic approximation instead predicts about a 4:7 ratio ($(0_0^0, 3_0^3) : (3_0^1, 3_0^2)$) and also produces a longer progression in the stretching mode (up to about $n' = 6$ or $n' = 7$). A direct comparison of the intensity pattern computed for this progression with experiment[1] is hampered by the somewhat low experimental resolution and overlapping signals due to additional photoprocesses, that have been attributed to a concomitant photodetachment-photoelectron spectrum of S_2^-, which is formed by photodissociation of the parent anionic compound.

The second prominent feature, which remained, however, unresolved in the experimental spectrum[1], is the progression $2_0^1 3_0^n$ that builds upon the excitation of the bending mode ν_2. The FCF for the 2_0^1 transition is in the deuterated species more pronounced than in the non-deuterated parent compound due to the larger projection of the change in equilibrium structure, that is caused by the electron detachment, onto the DS_2 bending mode.

Excitation in ν_1, the H-S or D-S stretching, mode are connected with very small FCFs (at most one per mil of the FCF of 0_0^0). This is primarily due to the almost negligible change of the corresponding bond length upon electron detachment, which is predicted by theory.

The computed FC profile of the photoelectron spectrum for the photodetachment process

that leads to the energetically lowest excited doublet state of HS_2 and DS_2 ($(\tilde{X}\ ^1A') \rightarrow (\tilde{X}\ ^2A'')$, see Figs. 3 and 4) reveals significantly less features. The main progression 2_0^n is due to the bending mode ν_2, but is very short and ends essentially at $n' = 2$. The most intense band is the 0_0^0 transition, with the other bands falling off rapidly in intensity. This is in good agreement with the experimental findings of Entfellner *et al.*.[1]

Excitations of the S-S stretching mode ν_3 are strongly suppressed due to the almost equal S-S bond length in the initial and final electronic state. The FCF of the 3_0^1 transition is only about 1/60 (1/15) of the FCF of 0_0^0 in HS_2 (DS_2). These bands were not resolvable in the experimental spectrum.

Even weaker is the computed 1_0^n progressions in the H-S and D-S stretching mode ν_1. The FCF obtained for 1_0^1 is only about one per mil of 0_0^0. Entfellner *et al.*[1] assigned, however, a signal in the corresponding wavenumber range to this transition. On the basis of our calculations, we can neither support nor fully rule out this assignment. While the wavenumber range matches, our computed intensity appears too low to justify the assignment. Due to the approximate nature of our calculation, however, where we neither included core-valence correlation effects nor relativistic corrections, the change in bond length upon electron detachment might be underestimated which will result in a too low bandstrength for this transition.

Overall, VSCF and VCI give quite similar FC profiles for the four photoelectron-photodetachment spectra. The VCI wavefunctions are for the most prominent bands usually dominated by a single reference, which also impacts on the resulting intensity pattern. A slightly more pronounced multi-configurational character is observed in particular when higher excitations of the bending mode are involved. Some strongly perturbed transitions are present in the photodetachment spectra of the deuterated species, where a close resonance situation is predicted for $1_0^1 3_0^2 / 2_0^1 3_0^4$ (and various progressions built on these) in the electron detachment spectrum that involves the electronic ground state of the radical. A similar situation occurs for $1_0^1 2_0^4 / 1_0^1 2_0^3 3_0^1$ in the corresponding $(\tilde{X}\ ^1A')DS_2^- \rightarrow (\tilde{A}\ ^2A')DS_2$ electronic transition.

Differences between harmonic and VSCF/VCI profiles are most prominent in the 3_0^n progressions (excitations of the S-S stretching mode) in the $(\tilde{X}\ ^1A') \rightarrow (\tilde{X}\ ^2A'')$ electron detachment process. The anharmonic progression is shorter than the harmonic one, which is not unexpected, as the S-S bond contracts upon removal of the electron. The details of

the profile depend on the shape of the potential function. We have to emphasise, however, that the underlying electronic structure calculations are difficult to converge for such large excursions from the equilibrium structure so that in particular the computed vibronic bands in the larger wavenumber region are to be considered as crude approximations. The corresponding data are thus intended primarily for facilitating the reproduction of our results. Given the current experimental resolution[1] for the photodetachment-photoelectron spectra of HS_2^- and DS_2^-, even the harmonic approximation might be considered a good starting point for the analysis.

V. SUMMARY, CONCLUSIONS AND OUTLOOK

We have reported herein the computed Franck–Condon profile for the photodetachment-photoelectron spectra of different isotopomers of disulfanide upon which the disulfanyl in its doublet ground and energetically lowest doublet excited state is formed. Three-dimensional anharmonic potential energy hypersurfaces have been computed in a fully automated fashion. Electronic structure calculations were performed at the explicitly correlated coupled clusters singles and doubles level with perturbative triples correction using a correlation-consistent polarized valence triple zeta atomic basis set[38,39]. The approach employed for the vibronic structure calculations combines VSCF/VCI wavefunctions in basis sets adapted to each electronic state, namely displaced Gaussian functions along the normal modes of each electronic state. The non-orthogonal basis functions require the calculation of multi-dimensional overlap integrals, but have the potential of supporting shorter VCI expansions and facilitating straight forward prescreening techniques.

The $(\tilde{X}\ ^1A') \rightarrow (\tilde{X}\ ^2A'')$ is dominated by excitations in the S-S stretching mode, whereas various weak additional features are due to an excitation of the bending mode. The computed FC profile is in reasonable agreement with the low-resolution spectrum obtained experimentally. As a result of smaller structural changes upon removal of the electron, the $(\tilde{X}\ ^1A') \rightarrow (\tilde{A}\ ^2A')$ transition is relatively featureless and contains a short progression in the bending mode as its main feature, which is in line with the experimental spectrum. Excitations in the S-S stretching mode are significantly less pronounced and remained unresolved in experiment. The single signal assigned in the experiment to an excitation of the H-S and D-S stretching mode, respectively, is computed to be extremely weak. Nevertheless,

the assignment can not be fully ruled out by virtue of the inherent approximation in the calculations.

While our initial application was limited to a three-dimensional vibronic problem, ongoing work will focus on the extension to medium sized systems.

VI. ACKNOWLEDGMENTS

RB acknowledges the Volkswagen Foundation for financial support and the Center for Scientific Computing (CSC) Frankfurt for computer time.

* Electronic address: rauhut@theochem.uni-stuttgart.de

† Electronic address: r.berger@fias.uni-frankfurt.de

[1] M. Entfellner and U. Boesl, Phys. Chem. Chem. Phys. **11**, 2657 (2009).

[2] S. Moran and G. Ellison, J. Phys. Chem. **92**, 1794 (1988).

[3] K. Peterson, A. Mitrushchenkov, and J. Francisco, Chem. Phys. **346**, 34 (2008).

[4] J. B. Coon, R. E. DeWames, and C. M. Loyd, J. Mol. Spectrosc. **8**, 285 (1962).

[5] T. Anno and A. Sado, J. Chem. Phys. **32**, 1611 (1960).

[6] W. L. Smith and P. A. Warsop, rans. Faraday Soc. **64**, 1165 (1968).

[7] T. E. Sharp and H. M. Rosenstock, J. Chem. Phys. **41**, 3453 (1964).

[8] R. Botter, V. H. Dibeler, J. A. Walker, and H. M. Rosenstock, J. Chem. Phys. **44**, 1271 (1966).

[9] H.-C. Jankowiak, J. L. Stuber, and R. Berger, J. Chem. Phys. **127**, 234101 (2007).

[10] F. Duschinsky, Acta Physicochim. URSS **7**, 551 (1937).

[11] F. Neese, Coord. Chem. Rev. **253**, 526 (2009).

[12] D. K. W. Mok, E. P. F. Lee, F.-T. Chau, D. C. Wang, and J. M. Dyke, J. Chem. Phys. **113**, 5791 (2000).

[13] J. M. Luis, B. Kirtman, and O. Christiansen, J. Chem. Phys. **125**, 154114 (2006).

[14] J. Bowman, X. Huang, L. Harding, and S. Carter, Mol. Phys. **104**, 33 (2006).

[15] V. Rodriguez-Garcia, K. Yagi, K. Hirao, S. Iwata, and S. Hirata, J. Chem. Phys. **125**, 014109 (2006).

[16] J. M. Bowman, T. Carrington, and H.-D. Meyer, Mol. Phys. **106**, 2145 (2008).

[17] P. Zielke, P. W. Forysinski, D. Luckhaus, and R. Signorell, J. Chem. Phys. **130**, 211101 (2009).

[18] M. Sparta, I. Hoyvik, D. Toffoli, and O. Christiansen, J. Phys. Chem. A **113**, 8712 (2009).

[19] M. Keceli, T. Shiozaki, K. Yagi, and S. Hirata, **107**, 1283 (2009).

[20] G. Rauhut, V. Barone, and P. Schwerdtfeger, J. Chem. Phys. **125**, 054308 (2006).

[21] S. Heislbetz, P. Schwerdtfeger, and G. Rauhut, Mol. Phys. **105**, 1385 (2007).

[22] S. Bonness, B. Kirtman, M. Huix, A. J. Sanchez, and J. M. Luis, J. Chem. Phys. **125**, 014311 (2006).

[23] M. Brommer, B. Weis, B. Follmeg, P. Rosmus, S. Carter, N. C. Handy, H.-J. Werner, and P. J. Knowles, J. Chem. Phys. **98**, 5222 (1993).

[24] G. Rauhut, J. Chem. Phys. **121**, 9313 (2004).

[25] T. Hrenar, H.-J. Werner, and G. Rauhut, J. Chem. Phys. **126**, 134108 (2007).

[26] J. Watson, Mol. Phys. **15**, 479 (1968).

[27] I. Hamilton and J. Light, J. Chem. Phys. **84**, 306 (1986).

[28] M. Neff and G. Rauhut, J. Chem. Phys. **000**, 0000 (2009).

[29] K. Pflüger, M. Paulus, S. Jagiella, T. Burkert, and G. Rauhut, Theor. Chem. Acc. **114**, 327 (2005).

[30] G. Rauhut and T. Hrenar, Chem. Phys. **346**, 160 (2008).

[31] G. Rauhut, G. Knizia, and H.-J. Werner, J. Chem. Phys. **130**, 054105 (2009).

[32] E. V. Doktorov, I. A. Malkin, and V. I. Man'ko, J. Mol. Spectrosc. **64**, 302 (1977).

[33] H.-J. Werner, T. B. Adler, and F. R. Manby, J. Chem. Phys. **126**, 164102 (2007).

[34] G. Knizia and H.-J. Werner, J. Chem. Phys. **128**, 154103 (2008).

[35] F. R. Manby, J. Chem. Phys. **119**, 4607 (2003).

[36] A. J. May and F. R. Manby, J. Chem. Phys. **121**, 4479 (2004).

[37] F. Weigend, A. Köhn, and C. Hättig, J. Chem. Phys. **116**, 3175 (2002).

[38] K. E. Yousaf and K. A. Peterson, J. Chem. Phys. **129**, 184108 (2008).

[39] T. B. Adler, G. Knizia, and H.-J. Werner, J. Chem. Phys. **127**, 221106 (2007).

[40] G. Knizia and H.-J. Werner, J. Chem. Phys. **128**, 154103 (2008).

[41] P. Carbonniere and V. Barone, Chem. Phys. Lett. **392**, 365 (2004).

[42] H.-J. Werner, P. J. Knowles, R. Lindh, F. R. Manby, M. Schütz, et al., *Molpro, development version 2008.3, a package of ab initio programs* (2008), see http://www.molpro.net.

[43] R. Berger, C. Fischer, and M. Klessinger, J. Phys. Chem. A **102**, 7157 (1998).

[44] J. S. Huh, H.-C. Jankowiak, J. L. Stuber, and R. Berger (to be published.).

[45] S. Ashworth and E. Fink, Mol. Phys. **105**, 715 (2007).

[46] E. Isoniemi, L. Khriachtchev, M. Petterson, and M. Räsänen, Chem. Phys. Lett. **311**, 47 (1999).

[47] K. Holstein, E. Fink, J. Wildt, and F. Zabel, Chem. Phys. Lett. **113**, 1 (1985).

[48] M. Tanimoto, T. Klaus, H. Müller, and G. Winnewisser, J. Mol. Spectr. **199**, 73 (2000).

Table I: Computed and observed fundamental vibrational wavenumbers (in cm^{-1}) of HS_2 and HS_2^-.

	$\tilde{X}^2A''$			$\tilde{A}^2A'$			$\tilde{X}^1A'$
	This work	PMF[a]	Exp.[b]	This work	PMF[a]	Exp.[b]	This work
r(HS)	1.3499	1.3482	1.3523	1.3435	1.3417		1.3472
R(SS)	1.9646	1.9608	1.9603	2.0807	2.0752		2.0883
$\theta(HSS)$	101.58	101.52	101.74	93.28	93.25		101.68
ω_1	2602.4	2598.3		2677.3	2674.1		2598.1
ω_2	918.7	919.0		771.9	770.5		831.5
ω_3	605.0	605.0		510.5	513.0		489.7
ν_1	2482.4	2474.5	2463	2569.7	2563.2	2550±200	2469.6
ν_2	898.2	900.8	904±8	752.6	752.8	750±200	809.7
ν_3	598.4	598.4	595±4	504.6	506.9	504±4	478.4

a) Taken from Peterson, Mitrushchenkov and Francisco, see Ref. 3

b) Experimental data taken from Refs. 45–48

Table II: Computed and observed fundamental vibrational wavenumbers (in cm^{-1}) of DS_2 and DS_2^-.

	$\tilde{X}^2A''$			$\tilde{A}^2A'$			$\tilde{X}^1A'$
	This work	PMF[a]	Exp.[b]	This work	PMF[a]	Exp.[b]	This work
ω_1	1869.6	1866.8		1922.4	1920.1		1866.5
ω_2	667.2	667.3		559.3	558.4		601.4
ω_3	603.4	603.6		508.6	511.0		484.6
ν_1	1807.5	1803.2		1866.1	1863.0	1830±160	1800.9
ν_2	656.6	657.9	696±20	549.0	549.0	540±160	589.6
ν_3	597.1	597.1	591±10	503.0	505.5	502±15	478.9

a) Taken from Peterson, Mitrushchenkov and Francisco, see Ref. 3

b) Experimental data taken from Refs. 45–48

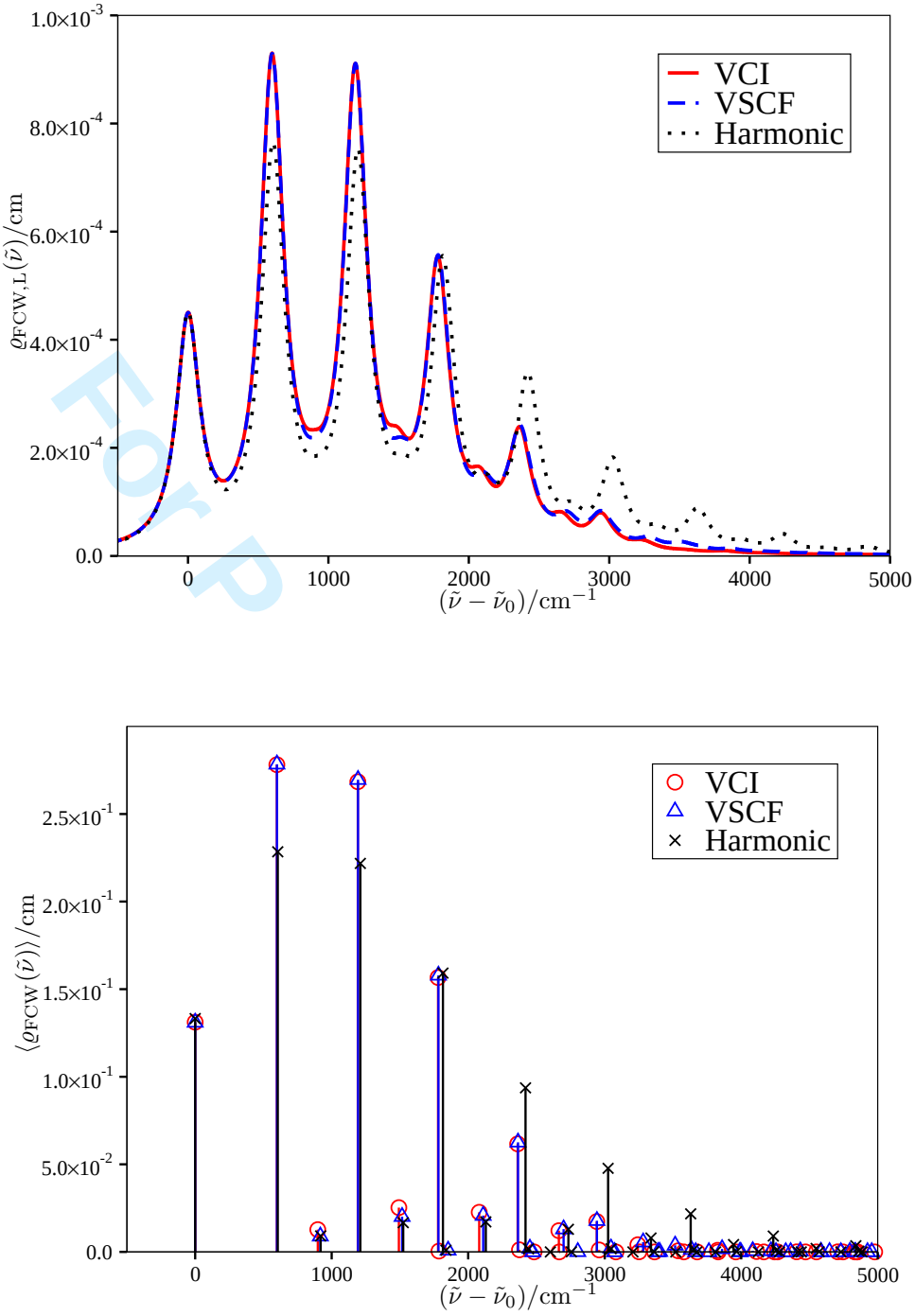

Figure 1: Franck–Condon profiles of the $(\tilde{\mathrm{X}}\ ^1\mathrm{A}')\mathrm{HS}_2^-$ → $(\tilde{\mathrm{X}}\ ^2\mathrm{A}'')\mathrm{HS}_2$ photodetachment-photoelectron spectrum computed in the harmonic approximation, the vibrational self-consistent field (VSCF) approximation and the vibrational configuration interaction (VCI) approximation. The lower graph shows a stick representation of the averaged Franck-Condon weighted density of states $\varrho_{\mathrm{FCW}}(\tilde{\nu})$ whereas the upper graph shows the corresponding profiles obtained after convolution with a Lorentzian lineshape function with full width at half maximum (FWHM) of 200 cm^{-1}.

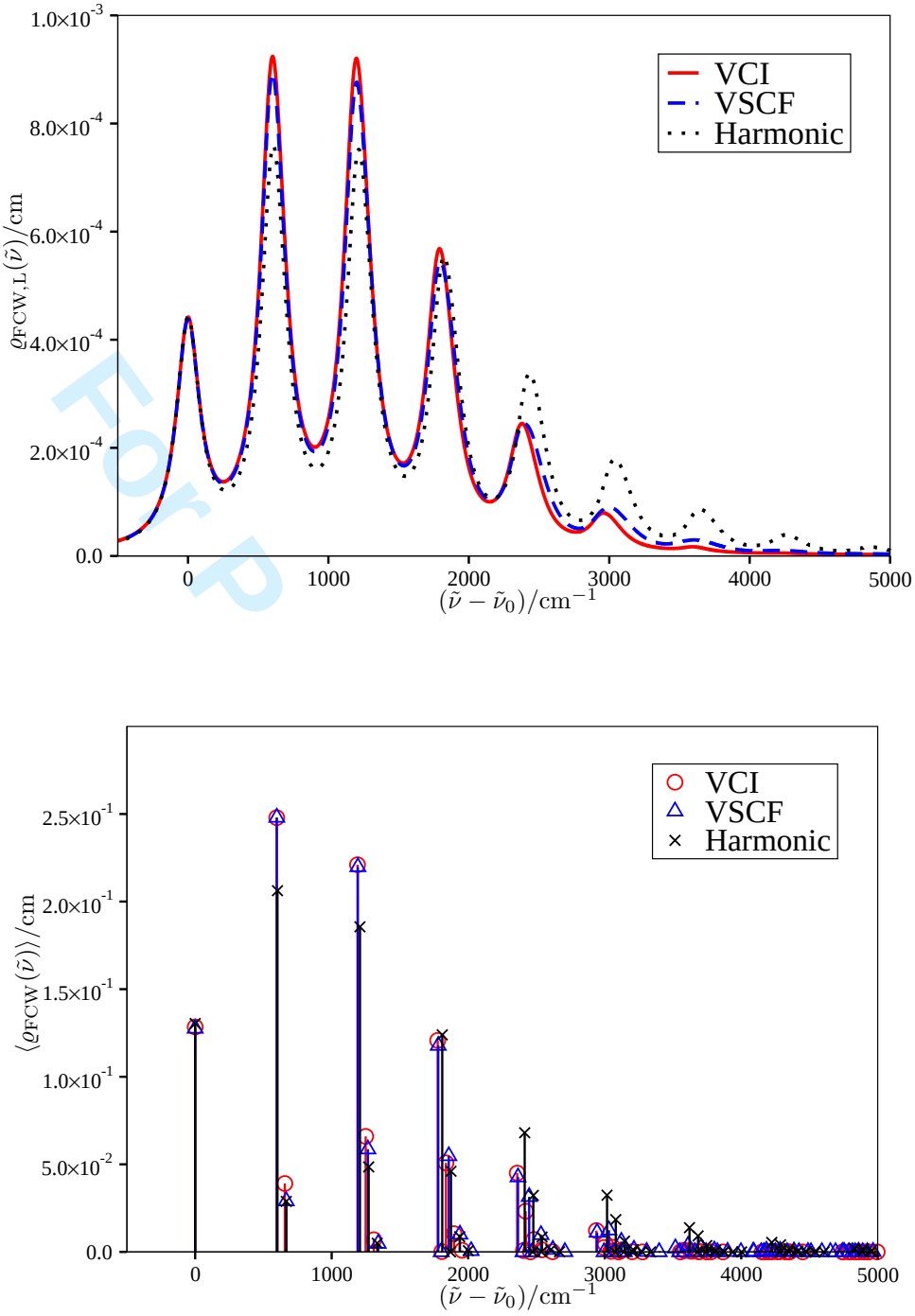

Figure 2: Franck–Condon profiles of the $(\tilde{\mathrm{X}}\ {}^1\mathrm{A}')\mathrm{DS}_2^-$ → $(\tilde{\mathrm{X}}\ {}^2\mathrm{A}'')\mathrm{DS}_2$ photodetachment-photoelectron spectrum computed in the harmonic approximation, the vibrational self-consistent field (VSCF) approximation and the vibrational configuration interaction (VCI) approximation. The lower graph shows a stick representation of the averaged Franck-Condon weighted density of states $\varrho_{\mathrm{FCW}}(\tilde{\nu})$ whereas the upper graph shows the corresponding profiles obtained after convolution with a Lorentzian lineshape function with FWHM of 200 cm^{-1}.

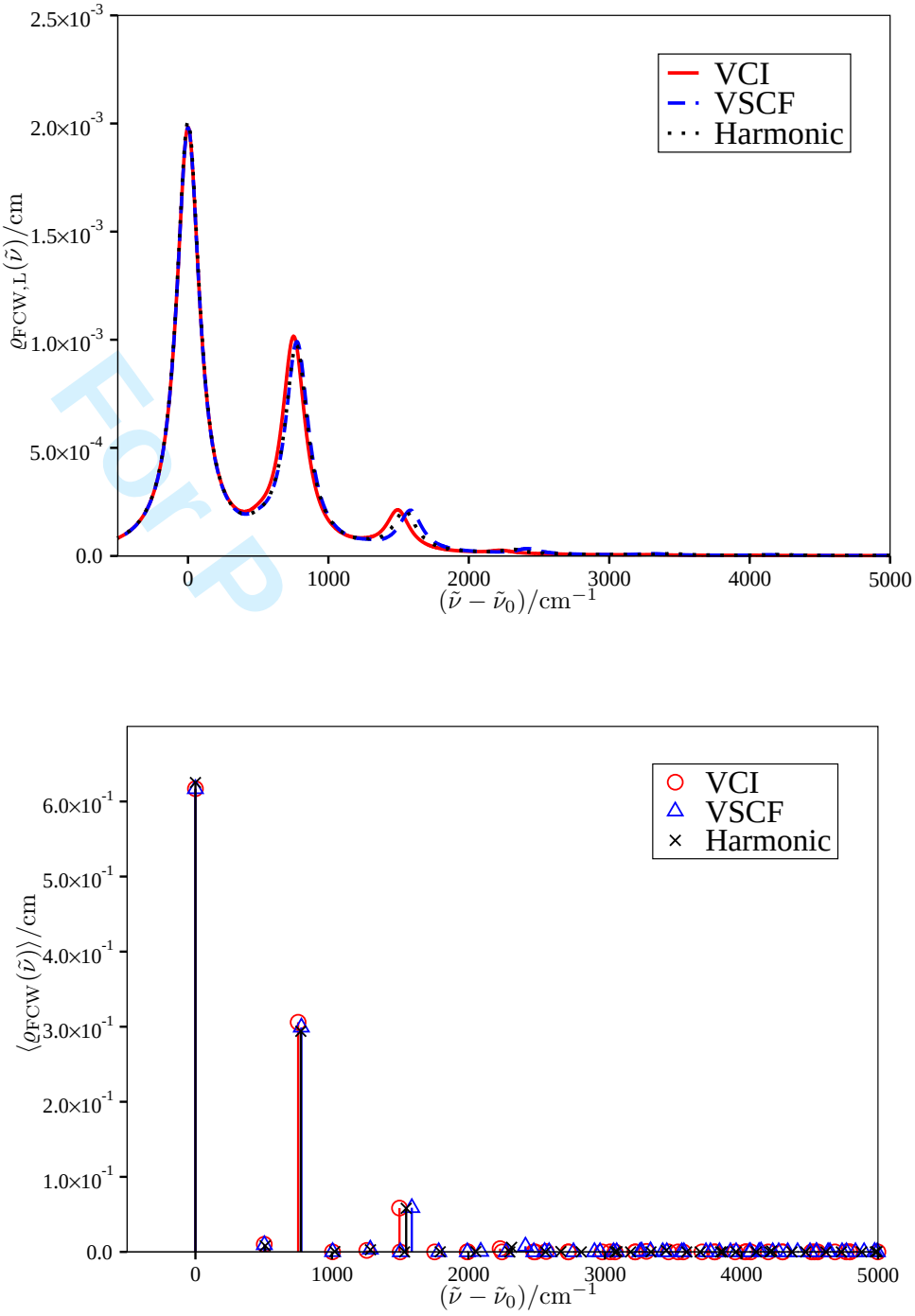

Figure 3: Franck–Condon profiles of the $(\tilde{\mathrm{X}}\ ^1\mathrm{A}')\mathrm{HS}_2^-$ → $(\tilde{\mathrm{A}}\ ^2\mathrm{A}')\mathrm{HS}_2$ photodetachment-photoelectron spectrum computed in the harmonic approximation, the vibrational self-consistent field (VSCF) approximation and the vibrational configuration interaction (VCI) approximation. The lower graph shows a stick representation of the averaged Franck-Condon weighted density of states $\varrho_{\mathrm{FCW}}(\tilde{\nu})$ whereas the upper graph shows the corresponding profiles obtained after convolution with a Lorentzian lineshape function with FWHM of 200 cm^{-1}.

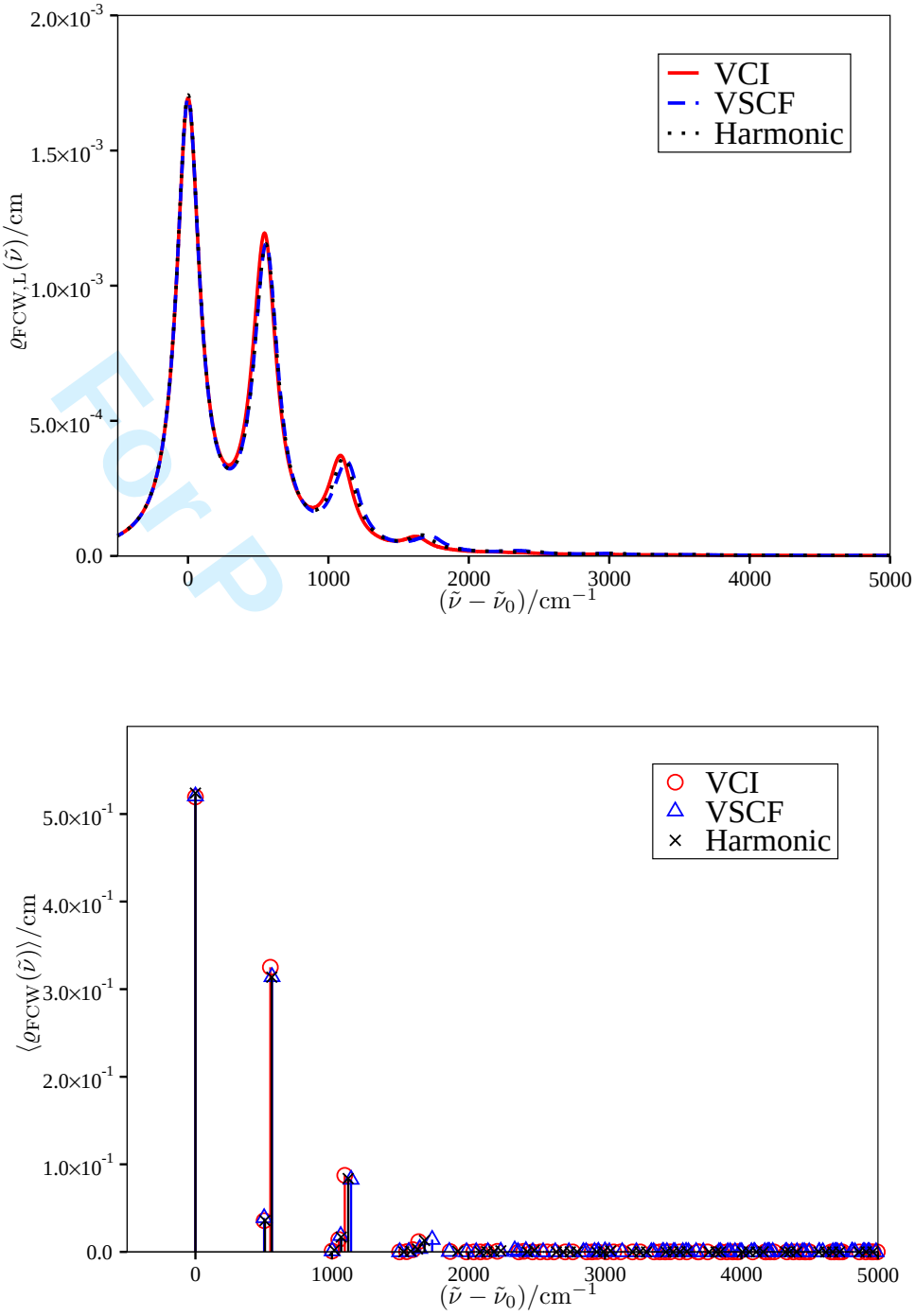

Figure 4: Franck–Condon profiles of the $(\tilde{\mathrm{X}}\ ^1\mathrm{A}')\mathrm{DS}_2^-$ → $(\tilde{\mathrm{A}}\ ^2\mathrm{A}')\mathrm{DS}_2$ photodetachment-photoelectron spectrum computed in the harmonic approximation, the vibrational self-consistent field (VSCF) approximation and the vibrational configuration interaction (VCI) approximation. The lower graph shows a stick representation of the averaged Franck-Condon weighted density of states $\varrho_{\mathrm{FCW}}(\tilde{\nu})$ whereas the upper graph shows the corresponding profiles obtained after convolution with a Lorentzian lineshape function with FWHM of 200 cm^{-1}.

Appendix A: BAND LISTING

Table III: Computed Franck-Condon factors (for a wavenumber range extending up to $\tilde{\nu} - \tilde{\nu}_0 < 4000$ cm^{-1}) and corresponding band assignments of the photodetachment process from HS_2^- ($\tilde{X}^1A'$) to ground state HS_2 ($\tilde{X}^2A''$). (a) Peak assignment based on harmonic oscillator wavefunctions (b) Peak assignment based on VSCF wavefunctions (c) Peak assignment for the VCI wavefunctions based on the (maximum) percentage contribution (numbers in parentheses) of the corresponding VSCF wave function.

Harmonic			VSCF			VCI		
ν_1 ν_2 ν_3 [a]	$\tilde{\nu} - \tilde{\nu}_0$	FCF	ν_1 ν_2 ν_3 [b]	$\tilde{\nu} - \tilde{\nu}_0$	FCF	ν_1 ν_2 ν_3 (%) [c]	$\tilde{\nu} - \tilde{\nu}_0$	FCF
0 0 0	0.00	1.33E-01	0 0 0	0.00	1.31E-01	0 0 0 (99.9)	0.00	1.31E-01
0 0 1	604.98	2.28E-01	0 0 1	599.14	2.78E-01	0 0 1 (99.8)	598.38	2.78E-01
0 1 0	918.73	9.12E-03	0 1 0	916.96	8.96E-03	0 1 0 (98.9)	898.29	1.27E-02
0 0 2	1209.96	2.22E-01	0 0 2	1193.05	2.70E-01	0 0 2 (99.8)	1191.51	2.68E-01
0 1 1	1523.71	1.67E-02	0 1 1	1516.10	2.01E-02	0 1 1 (98.4)	1492.16	2.53E-02
0 0 3	1814.94	1.59E-01	0 0 3	1781.72	1.58E-01	0 0 3 (99.7)	1779.39	1.57E-01
0 2 0	1837.46	9.38E-04	0 2 0	1852.80	8.68E-04	0 2 0 (94.7)	1785.99	4.83E-04
0 1 2	2128.69	1.71E-02	0 1 2	2110.01	2.08E-02	0 1 2 (98.0)	2080.82	2.26E-02
0 0 4	2419.92	9.37E-02	0 0 4	2365.14	6.26E-02	0 0 4 (99.6)	2362.08	6.17E-02
0 2 1	2442.44	1.73E-03	0 2 1	2451.95	1.98E-03	0 2 1 (93.1)	2375.21	1.19E-03
1 0 0	2602.40	2.54E-06	1 0 0	2472.92	1.12E-06	1 0 0 (96.9)	2482.42	5.53E-06
0 1 3	2733.67	1.29E-02	0 1 3	2698.68	1.30E-02	0 1 3 (97.2)	2664.25	1.21E-02
0 3 0	2756.19	7.30E-05	0 3 0	2802.89	5.96E-05	0 3 0 (87.5)	2666.94	1.72E-06
0 0 5	3024.90	4.77E-02	0 0 5	2943.29	1.78E-02	0 0 5 (99.7)	2941.73	1.74E-02
0 2 2	3047.42	1.80E-03	0 2 2	3045.85	2.07E-03	0 2 2 (91.7)	2959.32	1.12E-03
1 0 1	3207.38	3.99E-06	1 0 1	3072.06	2.10E-06	1 0 1 (96.3)	3082.35	5.90E-06
0 1 4	3338.65	7.95E-03	0 1 4	3282.10	5.56E-03	0 1 4 (97.0)	3242.78	4.10E-03
0 3 1	3361.17	1.39E-04	1 1 0	3389.88	5.36E-06	0 3 1 (84.8)	3251.56	2.31E-05
1 1 0	3521.13	6.82E-06	0 3 1	3402.03	1.44E-04	1 1 0 (90.4)	3365.17	1.20E-06
0 0 6	3629.88	2.18E-02	0 0 6	3516.18	3.76E-03	0 2 3 (90.4)	3538.26	6.49E-04
0 2 3	3652.40	1.37E-03	0 2 3	3634.52	1.32E-03	0 4 0 (80.7)	3579.96	1.02E-06
0 4 0	3674.92	6.00E-06	1 0 2	3665.97	1.78E-06	1 0 2 (95.8)	3676.99	1.97E-06
1 0 2	3812.36	3.57E-06	0 4 0	3763.19	3.78E-06	0 1 5 (96.6)	3826.60	9.63E-04
0 1 5	3943.63	4.22E-03	0 1 5	3860.25	1.72E-03	0 3 2 (81.4)	3831.30	1.48E-05
0 3 2	3966.15	1.48E-04	1 1 1	3989.02	1.13E-05	1 1 1 (89.6)	3960.72	1.84E-06
			0 3 2	3995.94	1.59E-04			

Table IV: Computed Franck-Condon factors (for a wavenumber range extending up to $\tilde{\nu} - \tilde{\nu}_0 < 4000$ cm^{-1}) and corresponding band assignments of the photodetachment process from HS_2^- ($\tilde{X}^1A'$) to the lowest excited doublet state of HS_2 ($\tilde{A}^2A'$). (a) Peak assignment based on harmonic oscillator wavefunctions (b) Peak assignment based on VSCF wavefunctions (c) Peak assignment for the VCI wavefunctions based on the (maximum) percentage contribution (numbers in parentheses) of the corresponding VSCF wavefunction.

Harmonic			VSCF			VCI		
ν_1 ν_2 ν_3 [a]	$\tilde{\nu} - \tilde{\nu}_0$	FCF	ν_1 ν_2 ν_3 [b]	$\tilde{\nu} - \tilde{\nu}_0$	FCF	ν_1 ν_2 ν_3 (%) [c]	$\tilde{\nu} - \tilde{\nu}_0$	FCF
0 0 0	0.00	6.25E-01	0 0 0	0.00	6.17E-01	0 0 0 (99.9)	0.00	6.17E-01
0 0 1	510.52	8.15E-03	0 0 1	504.86	9.35E-03	0 0 1 (99.8)	504.53	1.02E-02
0 1 0	771.91	2.94E-01	0 1 0	776.33	2.99E-01	0 1 0 (98.8)	752.59	3.06E-01
0 0 2	1021.04	4.65E-04	0 0 2	1005.23	1.92E-04	0 0 2 (99.8)	1004.52	6.49E-05
0 1 1	1282.43	2.83E-03	0 1 1	1281.18	3.42E-03	0 1 1 (98.7)	1254.83	2.01E-03
0 0 3	1531.56	1.09E-05	0 0 3	1501.07	1.39E-06	0 2 0 (94.8)	1495.01	5.84E-02
0 2 0	1543.82	5.80E-02	0 2 0	1585.30	5.88E-02	0 0 3 (99.7)	1499.93	1.04E-06
0 1 2	1792.95	1.79E-04	0 1 2	1781.56	6.19E-05	0 1 2 (98.5)	1752.29	9.15E-07
0 0 4	2042.08	4.42E-07	0 0 4	1992.37	2.64E-09	0 0 4 (99.6)	1990.79	8.97E-08
0 2 1	2054.34	3.63E-04	0 2 1	2090.16	4.55E-04	0 2 1 (94.4)	1994.97	2.03E-04
0 1 3	2303.47	3.43E-06	0 1 3	2277.40	3.29E-07	0 3 0 (88.2)	2232.08	4.44E-03
0 3 0	2315.73	6.08E-03	0 3 0	2418.17	7.47E-03	0 1 3 (98.2)	2244.93	1.65E-08
0 0 5	2552.60	1.19E-08	0 0 5	2479.37	3.31E-11	0 0 5 (99.6)	2478.07	1.95E-10
0 2 2	2564.86	2.81E-05	1 0 0	2557.85	1.86E-04	0 2 2 (94.0)	2489.93	2.46E-07
1 0 0	2677.34	5.73E-04	0 2 2	2590.54	6.99E-06	1 0 0 (98.1)	2569.62	5.36E-04
0 1 4	2813.99	1.47E-07	0 1 4	2768.69	1.77E-11	0 3 1 (87.4)	2730.01	2.83E-05
0 3 1	2826.25	1.86E-05	0 3 1	2923.02	3.29E-05	0 1 4 (97.8)	2733.31	1.41E-07
0 0 6	3063.12	4.23E-10	0 0 6	2963.91	1.03E-12	0 2 3 (93.4)	2979.84	6.37E-09
0 2 3	3075.38	3.92E-07	1 0 1	3062.71	3.89E-07	0 4 0 (83.3)	3037.67	8.43E-05
0 4 0	3087.64	3.44E-04	0 2 3	3086.38	2.33E-08	1 0 1 (98.0)	3073.72	4.66E-06
1 0 1	3187.86	2.71E-06	0 1 5	3255.69	1.96E-11	0 1 5 (97.3)	3220.20	9.36E-12
0 1 5	3324.51	3.43E-09	0 4 0	3268.03	8.78E-04	0 3 2 (86.3)	3222.95	2.20E-07
0 3 2	3336.77	2.24E-06	1 1 0	3334.18	1.28E-03	1 1 0 (93.0)	3303.62	7.19E-04
1 1 0	3449.25	2.00E-03	0 3 2	3423.40	4.21E-07	0 2 4 (93.1)	3465.95	4.96E-09
0 0 7	3573.64	1.20E-11	0 0 7	3453.01	6.92E-13	0 4 1 (82.6)	3534.95	6.53E-06
0 2 4	3585.90	1.92E-08	1 0 2	3563.08	3.02E-09	1 0 2 (97.9)	3573.32	6.92E-08
0 4 1	3598.16	1.61E-07	0 2 4	3577.67	1.28E-10	0 3 3 (85.8)	3710.80	1.39E-09
1 0 2	3698.38	2.28E-07	0 1 6	3740.24	1.26E-12	0 5 0 (74.9)	3801.82	1.06E-06
0 1 6	3835.03	1.25E-10	0 4 1	3772.89	1.78E-06	1 1 1 (92.5)	3805.88	1.22E-06
0 3 3	3847.29	1.69E-08	1 1 1	3839.03	1.26E-05	0 2 5 (93.0)	3953.55	8.96E-10
0 5 0	3859.55	8.73E-06	0 3 3	3919.24	5.87E-10			
1 1 1	3959.77	1.68E-05	0 0 8	3960.83	2.04E-13			

Table V: Computed Franck-Condon factors (for a wavenumber range extending up to $\tilde{\nu} - \tilde{\nu}_0 < 4000$ cm^{-1}) and corresponding band assignments of the photodetachment process from DS_2^- ($\tilde{X}^1A'$) to ground state DS_2 ($\tilde{X}^2A''$). (a) Peak assignment based on harmonic oscillator wavefunctions (b) Peak assignment based on VSCF wavefunctions (c) Peak assignment for the VCI wavefunctions based on the (maximum) percentage contribution (numbers in parentheses) of the corresponding VSCF wave function.

Harmonic			VSCF			VCI		
ν_1 ν_2 ν_3[a]	$\tilde{\nu} - \tilde{\nu}_0$	FCF	ν_1 ν_2 ν_3[b]	$\tilde{\nu} - \tilde{\nu}_0$	FCF	ν_1 ν_2 ν_3 (%)[c]	$\tilde{\nu} - \tilde{\nu}_0$	FCF
0 0 0	0.00	1.30E-01	0 0 0	0.00	1.28E-01	0 0 0 (99.9)	0.00	1.28E-01
0 0 1	603.44	2.06E-01	0 0 1	598.38	2.48E-01	0 0 1 (99.7)	597.08	2.48E-01
0 1 0	667.15	2.88E-02	0 1 0	666.53	2.91E-02	0 1 0 (99.2)	656.57	3.91E-02
0 0 2	1206.88	1.86E-01	0 0 2	1191.91	2.20E-01	0 0 2 (99.6)	1189.24	2.21E-01
0 1 1	1270.59	4.85E-02	0 1 1	1264.91	5.87E-02	0 1 1 (98.0)	1249.11	6.59E-02
0 2 0	1334.30	4.97E-03	0 2 0	1340.97	4.81E-03	0 2 0 (96.1)	1308.27	6.96E-03
0 0 3	1810.32	1.24E-01	0 0 3	1780.63	1.18E-01	0 0 3 (99.5)	1776.42	1.21E-01
1 0 0	1869.60	3.56E-07	1 0 0	1802.77	6.05E-08	1 0 0 (97.4)	1807.43	1.71E-04
0 1 2	1874.03	4.61E-02	0 1 2	1858.45	5.48E-02	0 1 2 (96.8)	1837.10	5.08E-02
0 2 1	1937.74	8.68E-03	0 2 1	1939.35	1.00E-02	0 2 1 (92.9)	1896.05	1.04E-02
0 3 0	2001.45	7.17E-04	0 3 0	2022.01	6.20E-04	0 3 0 (90.8)	1956.35	8.95E-04
0 0 4	2413.76	6.80E-02	0 0 4	2364.55	4.27E-02	0 0 4 (99.2)	2359.02	4.50E-02
1 0 1	2473.04	1.32E-07	1 0 1	2401.14	4.71E-09	1 0 1 (92.6)	2404.36	7.71E-04
0 1 3	2477.47	3.22E-02	0 1 3	2447.16	3.15E-02	0 1 3 (93.0)	2420.77	2.32E-02
1 1 0	2536.75	3.95E-06	1 1 0	2469.30	3.01E-06	1 1 0 (91.7)	2455.84	6.05E-05
0 2 2	2541.18	8.51E-03	0 2 2	2532.88	9.77E-03	0 2 2 (89.8)	2479.75	7.06E-03
0 3 1	2604.89	1.29E-03	0 3 1	2620.39	1.36E-03	0 3 1 (85.5)	2539.76	1.21E-03
0 4 0	2668.60	9.33E-05	0 4 0	2708.44	6.67E-05	0 4 0 (85.6)	2618.72	7.83E-05
0 0 5	3017.20	3.24E-02	0 0 5	2943.71	1.11E-02	0 0 5 (98.9)	2938.92	1.22E-02
1 0 2	3076.48	5.40E-10	1 0 2	2994.68	2.13E-07	1 0 2 (59.8)	2994.23	2.47E-03
0 1 4	3080.91	1.85E-02	0 1 4	3031.08	1.24E-02	0 1 4 (61.4)	3003.10	4.74E-03
1 1 1	3140.19	5.42E-06	1 1 1	3067.68	4.96E-06	1 1 1 (77.0)	3046.89	2.97E-04
0 2 3	3144.62	6.13E-03	0 2 3	3121.60	5.90E-03	0 2 3 (78.7)	3060.10	2.65E-03
1 2 0	3203.90	1.57E-06	1 2 0	3143.74	1.25E-06	1 2 0 (80.9)	3101.68	1.32E-05
0 3 2	3208.33	1.30E-03	0 3 2	3213.92	1.41E-03	0 3 2 (80.3)	3119.49	7.27E-04
0 4 1	3272.04	1.73E-04	0 4 1	3306.82	1.56E-04	0 4 1 (78.0)	3201.42	9.65E-05
0 5 0	3335.75	1.12E-05	0 5 0	3399.15	5.88E-06	0 5 0 (78.8)	3276.91	8.12E-06
0 0 6	3620.64	1.38E-02	0 0 6	3518.15	2.15E-03	2 0 0 (95.3)	3554.86	4.65E-06
1 0 3	3679.92	4.77E-08	2 0 0	3548.87	1.99E-07	0 1 5 (53.5)	3579.13	9.46E-04
0 1 5	3684.35	9.13E-03	1 0 3	3583.40	4.04E-07	1 0 3 (54.0)	3589.49	8.57E-04
2 0 0	3739.20	5.16E-08	0 1 5	3610.24	3.58E-03	0 2 4 (46.9)	3629.74	4.16E-04
1 1 2	3743.63	4.23E-06	1 1 2	3661.21	3.63E-06	1 1 2 (48.0)	3641.86	4.49E-04
0 2 4	3748.06	3.61E-03	0 2 4	3705.52	2.47E-03	1 2 1 (53.7)	3687.48	7.35E-05
1 2 1	3807.34	2.41E-06	1 2 1	3742.11	2.29E-06	0 3 3 (57.5)	3697.04	2.03E-04
0 3 3	3811.77	9.64E-04	0 3 3	3802.64	9.04E-04	1 3 0 (70.1)	3746.91	4.08E-07
1 3 0	3871.05	3.87E-07	1 3 0	3824.78	2.90E-07	0 4 2 (72.9)	3779.90	5.49E-05
0 4 2	3875.48	1.79E-04	0 4 2	3900.36	1.73E-04	0 5 1 (73.2)	3865.65	1.01E-05
0 5 1	3939.19	2.13E-05	0 5 1	3997.53	1.49E-05			

Table VI: Computed Franck-Condon factors (for a wavenumber range extending up to $\tilde{\nu} - \tilde{\nu}_0 < 4000$ cm^{-1}) and corresponding band assignments of the photodetachment process from DS_2^- ($\tilde{X}^1A'$) to the lowest excited doublet state of DS_2 ($\tilde{A}^2A'$). (a) Peak assignment based on harmonic oscillator wavefunctions (b) Peak assignment based on VSCF wavefunctions (c) Peak assignment for the VCI wavefunctions based on the (maximum) percentage contribution (numbers in parentheses) of the corresponding VSCF wavefunction.

Harmonic			VSCF			VCI		
ν_1 ν_2 ν_3 [a]	$\tilde{\nu} - \tilde{\nu}_0$	FCF	ν_1 ν_2 ν_3 [b]	$\tilde{\nu} - \tilde{\nu}_0$	FCF	ν_1 ν_2 ν_3 (%) [c]	$\tilde{\nu} - \tilde{\nu}_0$	FCF
0 0 0	0.00	5.24E-01	0 0 0	0.00	5.20E-01	0 0 0 (99.9)	0.00	5.19E-01
0 0 1	508.59	3.58E-02	0 0 1	503.10	3.89E-02	0 0 1 (99.8)	502.95	3.57E-02
0 1 0	559.34	3.14E-01	0 1 0	560.95	3.14E-01	0 1 0 (99.2)	549.03	3.25E-01
0 0 2	1017.18	2.01E-03	0 0 2	1001.77	1.01E-03	0 0 2 (99.7)	1001.37	9.89E-04
0 1 1	1067.93	1.69E-02	0 1 1	1064.05	1.85E-02	0 1 1 (98.9)	1050.14	1.41E-02
0 2 0	1118.68	8.38E-02	0 2 0	1140.33	8.27E-02	0 2 0 (96.3)	1093.75	8.74E-02
0 0 3	1525.77	9.47E-05	0 0 3	1495.98	1.04E-05	0 0 3 (99.6)	1495.25	1.44E-05
0 1 2	1576.52	8.17E-04	0 1 2	1562.72	2.34E-04	0 1 2 (98.4)	1546.64	2.39E-04
0 2 1	1627.27	3.32E-03	0 2 1	1643.43	3.71E-03	0 2 1 (95.6)	1593.15	2.59E-03
0 3 0	1678.02	1.30E-02	0 3 0	1734.01	1.41E-02	0 3 0 (91.4)	1634.89	1.17E-02
1 0 0	1922.38	7.41E-04	1 0 0	1860.01	3.35E-04	1 0 0 (98.7)	1866.13	4.17E-04
0 0 4	2034.36	4.07E-06	0 0 4	1985.72	2.09E-08	0 0 4 (99.3)	1984.64	8.41E-08
0 1 3	2085.11	3.32E-05	0 1 3	2056.93	1.63E-07	0 1 3 (97.6)	2038.53	2.29E-06
0 2 2	2135.86	1.35E-04	0 2 2	2142.10	9.09E-06	0 2 2 (94.5)	2087.90	2.68E-05
0 3 1	2186.61	3.40E-04	0 3 1	2237.11	4.47E-04	0 3 1 (90.6)	2132.66	3.07E-04
0 4 0	2237.36	1.29E-03	0 4 0	2338.65	2.00E-03	0 4 0 (87.8)	2211.51	6.86E-04
1 0 1	2430.97	9.74E-05	1 0 1	2363.11	5.87E-05	1 0 1 (98.5)	2368.59	4.88E-07
1 1 0	2481.72	1.85E-03	1 1 0	2420.96	1.23E-03	1 1 0 (94.8)	2405.57	7.01E-04
0 0 5	2542.95	1.63E-07	0 0 5	2470.98	4.11E-11	0 0 5 (99.1)	2469.53	2.99E-10
0 1 4	2593.70	1.25E-06	0 1 4	2546.67	2.06E-08	0 1 4 (96.9)	2526.25	3.29E-09
0 2 3	2644.45	4.54E-06	0 2 3	2636.31	4.13E-07	0 2 3 (93.2)	2578.01	1.81E-07
0 3 2	2695.20	1.13E-05	0 3 2	2735.78	6.37E-07	0 3 2 (89.5)	2625.82	2.64E-06
0 4 1	2745.95	1.75E-05	0 4 1	2841.75	4.04E-05	0 4 1 (87.3)	2708.65	2.21E-05
0 5 0	2796.70	8.14E-05	1 0 2	2861.78	2.44E-06	0 5 0 (81.1)	2764.00	8.53E-06
1 0 2	2939.56	7.31E-06	1 1 1	2924.06	1.25E-04	1 0 2 (98.2)	2866.53	6.61E-08
1 1 1	2990.31	1.63E-04	0 5 0	2951.40	2.75E-04	1 1 1 (94.1)	2906.16	1.01E-06
1 2 0	3041.06	1.22E-03	0 0 6	2951.74	2.68E-14	1 2 0 (85.3)	2942.37	3.85E-04
0 0 6	3051.54	6.15E-09	1 2 0	3000.35	8.88E-04	0 1 5 (97.0)	3009.74	1.45E-11
0 1 5	3102.29	4.39E-08	0 1 5	3031.93	3.06E-10	0 2 4 (91.9)	3064.19	1.80E-10
0 2 4	3153.04	1.44E-07	0 2 4	3126.05	1.13E-08	0 3 3 (88.1)	3114.45	1.69E-08
0 3 3	3203.79	2.82E-07	0 3 3	3229.99	2.61E-07	0 4 2 (86.5)	3201.27	1.38E-07
0 4 2	3254.54	4.45E-07	0 4 2	3340.42	1.01E-06	0 5 1 (80.5)	3260.05	1.21E-06
0 5 1	3305.29	2.87E-07	1 0 3	3356.00	3.52E-08	1 0 3 (97.9)	3359.94	1.40E-09
0 6 0	3356.04	3.11E-06	1 1 2	3422.73	3.18E-06	1 1 2 (93.2)	3402.18	6.70E-08
1 0 3	3448.15	4.37E-07	0 0 7	3428.04	1.33E-14	1 2 1 (83.9)	3441.27	3.09E-07
1 1 2	3498.90	9.82E-06	0 5 1	3454.50	3.07E-06	1 3 0 (72.4)	3478.25	9.58E-05
1 2 1	3549.65	7.83E-05	1 2 1	3503.45	6.38E-05	0 2 5 (93.1)	3546.95	1.32E-12
0 0 7	3560.13	2.23E-10	0 1 6	3512.69	1.06E-12	0 3 4 (87.3)	3599.36	1.63E-10
1 3 0	3600.40	3.81E-04	0 6 0	3569.63	3.58E-05	2 0 0 (97.5)	3679.94	2.53E-05
0 1 6	3610.88	1.46E-09	1 3 0	3594.02	2.93E-04	0 4 3 (85.6)	3689.43	6.87E-10
0 2 5	3661.63	4.21E-09	0 2 5	3611.31	2.41E-13	0 5 2 (79.9)	3751.82	7.75E-09
0 3 4	3712.38	6.95E-09	2 0 0	3668.37	1.42E-04	1 0 4 (97.6)	3848.88	5.31E-11
0 4 3	3763.13	6.13E-09	0 3 4	3719.73	2.71E-10	1 1 3 (92.1)	3893.61	4.99E-10
0 5 2	3813.88	5.09E-09	0 4 3	3834.64	4.82E-08	1 2 2 (82.1)	3935.53	4.71E-08
2 0 0	3844.76	8.12E-05	1 0 4	3845.74	1.23E-10	1 4 0 (64.6)	3968.04	1.95E-06
0 6 1	3864.63	1.69E-09	0 0 8	3899.91	2.25E-15	1 3 1 (61.2)	3977.48	1.56E-06
0 7 0	3915.38	5.71E-08	1 1 3	3916.95	1.76E-08			
1 0 4	3956.74	2.25E-08	0 5 2	3953.17	3.17E-07			
			0 1 7	3988.99	1.54E-14			